Genome-wide signals of drift and local adaptation during rapid lineage divergence in a songbird

Running title: Drift and selection in a songbird radiation

Guillermo Friis,[1] Guillermo Fandos,[2] Amanda Zellmer,[3] John McCormack,[3,4] Brant Faircloth,[5] Borja Milá[1]

[1]National Museum of Natural Sciences, Spanish National Research Council (CSIC), Madrid 28006, Spain; [2]Department of Biodiversity, Ecology and Evolution, Complutense University of Madrid, Madrid 28040, Spain; [3]Department of Biology, Occidental College, Los Angeles, CA 90041, USA; [4]Moore Laboratory of Zoology and Department of Biology, Occidental College, Los Angeles, CA 90041, USA; [5]Department of Biological Sciences and Museum of Natural Science, Louisiana State University, Baton Rouge, LA 70803, USA

Corresponding author: Guillermo Friis, National Museum of Natural Sciences - CSIC, José Gutiérrez Abascal 2, Madrid 28006, Spain; Email: gfriis@mncn.csic.es; Tel: +34 914111328 x1266.

Abstract

The formation of independent evolutionary lineages involves neutral and selective factors, and understanding their relative roles in population divergence is a fundamental goal of speciation research. Correlations between allele frequencies and environmental variability can reveal the role of selection, yet the relative contribution of drift can be difficult to establish. Recently diversified systems such as that of the Oregon junco (Aves: Emberizidae) of western North America provide ideal scenarios to apply genetic-environment association analyses (GEA) while controlling for population structure. Genome-wide SNP loci analyses revealed marked genetic structure consisting of differentiated populations in isolated, dry southern mountain ranges, and more admixed recently expanded populations in humid northern latitudes. We used correlations between genomic and environmental variance to test for three specific modes of evolutionary divergence: (i) drift in geographic isolation, (ii) differentiation along continuous selective gradients, and (iii) isolation by adaptation. We found evidence of strong drift in southern mountains, but also signals of local adaptation in several populations, driven by temperature, precipitation, elevation and vegetation, especially when controlling for population history. We identified numerous variants under selection scattered across the genome, suggesting that local adaptation can promote rapid differentiation over short periods when acting over multiple independent loci.

Key words: local adaptation, isolation by adaptation, drift, selective gradients, redundancy analysis, postglacial expansion

Introduction

Lineage diversification involves both selective and neutral factors, and elucidating their relative strengths and interactions in the process of evolutionary divergence is essential to understand the mechanisms underlying the early stages of speciation (Coyne and Orr 2004; Nosil 2012). Lineage differentiation can be driven by divergent natural selection (Darwin 1859; Coyne and Orr 2004), a mechanism that is at the core of 'ecological speciation' models, in which reproductive isolation arises as a by-product of cumulative, ecologically adaptive changes (Mayr 1947; Schluter 2000; Rundle and Nosil 2005). In turn, accumulation of genetic differences caused by drift in geographic isolation or in isolation-by-distance (IBD, Wright 1943; Wright 1946) has been proposed as a mode of divergence driven by neutral factors (Mayr 1954, 1963), a mechanism that can be particularly strong in populations of small effective size (e.g. Carson 1975; Templeton 1981; Uyeda et al. 2009). Selection and drift can also act jointly and even interact during evolutionary divergence in a number of ways. Geographic distance usually implies environmental differences that may drive adaptation to local conditions and ecological differentiation, even if populations are connected by moderate gene flow (Schluter 2000; Rundle and Nosil 2005). The evolution of local adaptation can in turn result in isolation-by-adaptation (IBA), a mode of divergence where adaptive changes lead to intrinsic barriers to gene flow, enabling genome-wide differentiation at both neutral and selected loci (Nosil et al. 2008; Funk et al. 2011). Consequently, geographic distance and ecological divergence may promote similar patterns of genetic diversity among populations, so that teasing apart the roles of neutral evolution and ecological adaptation in evolutionary diversification requires approaches that account for both environmental heterogeneity and neutral population

68 structure (Wang and Bradburd 2014; Frichot et al. 2015; Rellstab et al. 2015; Forester et
69 al. 2016).
70
71 Our capacity to assess the relative roles of adaptation and neutral differentiation in
72 driving population divergence has benefitted from our increased ability to survey
73 genome-wide variation thanks to the development of next generation sequencing (NGS)
74 techniques (McCormack et al. 2013; Faria et al. 2014). The increasingly large number
75 of loci afforded by NGS provides improved resolution to detect neutral population
76 structure and patterns of gene flow among differentiated lineages. In addition, highly
77 differentiated loci identified as outliers in an F_{ST} distribution can be interpreted as
78 potential targets of divergent selection standing out in a background of balanced or
79 neutrally maintained genomic variation (Faria et al. 2014; Rellstab et al. 2015).
80 However, methods of outlier detection relying solely on allele frequencies are sensitive
81 to the confounding effects of historical factors, such as past sudden changes in
82 population size or strong drift in small populations that may result in high rates of false
83 positives (Edmonds et al. 2004; Kawecki and Ebert 2004; Billiard et al. 2005; Christmas
84 et al. 2016). Moreover, changes in allele frequencies due to local adaptation can
85 sometimes go undetected by outlier analyses (Pritchard and Di Rienzo 2010; Bierne et
86 al. 2011; Rellstab et al. 2015; Forester et al. 2017). Alternative approaches that integrate
87 environmental parameters by identifying allele frequencies that correlate with
88 ecological variability have proven useful to detect signals of adaptation, especially when
89 selective forces are weak (Frichot et al. 2015; Rellstab et al. 2015; Forester et al. 2017).
90 These methods, known as genetic-environment association (GEA, Hedrick et al. 1976;
91 Mitton et al. 1977) analyses, have the potential to reveal genetic patterns of
92 differentiation due to local adaptation while testing for the role of multiple, specific

93 environmental variables as drivers of selection (Forester et al. 2017). Importantly, GEA
94 methods can correct for population history by controlling for general patterns of neutral
95 genomic variation (Rellstab et al. 2015; Forester et al. 2016), allowing us to separate the
96 respective effects of drift and selection in generating and maintaining variability. GEA
97 analyses have greatly benefitted from the development of high-throughput sequencing
98 techniques, resulting in a number of studies focusing on the genomic variability
99 associated with environmental parameters in groups as diverse as plants (Lasky et al.
100 2012; Jones et al. 2013; De Kort et al. 2014; Nadeau et al. 2016; Sork et al. 2016),
101 fungus (Ojeda Alayon et al. 2017), wolves (Forester et al. 2017) and birds (Manthey and
102 Moyle 2015; Safran et al. 2016; Szulkin et al. 2016; Termignoni-García et al. 2017).
103
104 Recently diversified systems provide an ideal scenario for studying the relative roles of
105 selective and neutral factors in incipient divergence and speciation. Specifically, GEA
106 methods are particularly suitable when the system under study (i) is composed of
107 closely related populations, among which the signals of selection are still recent and
108 detectable; (ii) includes broad geographic distributions encompassing heterogeneous
109 habitats across ecological clines (*i.e.* selective gradients) but also spatially
110 discontinuous habitats so that adaptive and neutral divergence can be assessed in
111 different spatial settings; (iii) shows large variability in the degree of geographical
112 isolation among populations, from extensive gene flow to total isolation; and (iv)
113 presents low variability in secondary sexual traits so that differential sexual selection
114 can be ruled out as a major driver of population divergence.
115
116 The Oregon junco complex (*Junco hyemalis oreganus*) of western North America
117 provides a particularly well suited system to carry out genome-environment association

118 analysis. The complex originated recently as part of the postglacial radiation of dark-
119 eyed juncos across North America following a northward recolonization of the
120 continent as ice sheets retreated after the last glacial maximum, c.a. 18,000 years ago
121 (Milá et al. 2007; Friis et al. 2016; Milá et al. 2016). Among dark-eyed junco forms, the
122 Oregon junco group presents the highest variability in terms of phenotype and
123 ecological range, encompassing a broad latitudinal range from Baja California to Alaska
124 (Fig. 1A). All forms of the Oregon junco share a characteristic dark hood, yet there is
125 considerable population variation in plumage color, mainly of the hood, dorsum and
126 flanks, and the complex has been traditionally divided into at least 7 subspecific forms
127 (Dwight 1918; Miller 1941; Nolan et al. 2002), which include, from south to north:
128 *townsendi*, from the San Pedro Mártir mountains in northern Baja California, Mexico;
129 *pontilis*, distributed just north of *townsendi* in the Sierra Juárez mountains, also in Baja
130 California, Mexico; *thurberi*, from the mountains of southern California and Sierra
131 Nevada; *pinosus*, a coastal form from central California, predominantly distributed in
132 the Santa Cruz mountains; *montanus*, distributed across the interior of Oregon,
133 Washington and British Columbia; *shufeldti*, a more coastal form from Oregon and
134 Washington; and *oreganus* from coastal British Columbia and southern Alaska (Miller
135 1941; Nolan et al. 2002; Fig. 1A, Fig. 2A, Table 1).
136
137 The diverse spatial configuration of populations and environmental variability across
138 the Oregon junco distribution are critical aspects that will affect our capacity to
139 disentangle the roles of adaptive and neutral factors in explaining genomic variance.
140 Here we use a conceptual framework to classify into three main settings the distinct
141 spatial scenarios observable in the Oregon junco with respect to gene flow and
142 environmental variation. These include (i) geographically isolated populations in similar

143 habitats, as in the case of the Baja California *townsendi* and *pontilis* forms, where low
144 levels of local adaptation and low rates of gene flow should result in limited adaptive
145 divergence and high neutral divergence by drift (Fig. 2A); (ii) parapatric populations
146 under divergent ecological conditions, as exemplified by the *pinosus* and *thurberi* forms
147 in California, where divergence is expected to increase due to local adaptation, while
148 geographic proximity and moderate gene flow should lead to intermediate levels of
149 neutral differentiation by drift (Fig. 2B); and (iii) populations found along a continuous
150 environmental gradient, as in the northernmost forms of Oregon junco (*thurberi*,
151 *shufeldti*, *montanus* and *oreganus*) where neutral divergence is expected to be low due
152 to high levels of gene flow, while local adaptation along the gradient may result in a
153 pattern of high differentiation in adaptive variation (Fig. 2C).
154
155 Here we use the Oregon junco complex to study how geographic isolation, population
156 history, and local ecological adaptation have driven population differentiation across the
157 range, using extensive population sampling and genome-wide SNPs obtained from
158 'genotyping by sequencing' (GBS, Elshire et al. 2011). A draft consensus genome of
159 junco has also been sequenced and assembled to be used as a reference. We first assess
160 patterns of neutral genetic structure across the complex using selectively neutral SNPs,
161 and we then look for correlations between environmental variables and allele
162 frequencies across the Oregon junco distribution using redundancy analysis (RDA). We
163 also use climatic variables to test for significant niche divergence while controlling for
164 spatial autocorrelation. Finally, we map GBS sequences harboring significant outlier
165 SNP loci to the zebra finch (*Taeniopygia guttata*) reference genome in order to recover
166 the chromosomal position of polymorphic sites and explore how adaptive variation is
167 distributed across the genome.

Materials and methods

Population sampling

Oregon junco populations were sampled across the geographical range of the species using mist nets in order to obtain biological samples for DNA extraction (Fig. 1A). Each captured individual was aged, sexed, and marked with a numbered aluminum band. A blood sample was collected by venipuncture of the sub-brachial vein and stored in Queen's lysis buffer (Seutin 1991) or absolute ethanol at -80ºC in the laboratory. All sampling activities were conducted in compliance with Animal Care and Use Program regulations at the University of California Los Angeles, and with state and federal scientific collecting permits in the USA and Mexico. A high-quality tissue sample for whole-genome sequencing was obtained from a red-backed junco (*J. hyemalis dorsalis*) specimen (MLZ 69090) provided by the Moore Laboratory of Zoology, Occidental College, that was collected at Dude Mountain, Coconino County, Arizona. Genomic DNA was extracted from blood and tissue samples using a Qiagen DNeasy kit (Qiagen™, Valencia, CA).

Whole-genome sequencing and assembly

We assembled a draft dark-eyed junco genome by combining low-coverage genomes of eight different junco individuals, which we then used as a conspecific reference in the SNP calling process. Libraries for seven of the genomes were prepared with the Kapa Library Preparation Kit (Kapa Biosystems, Inc.) using TruSeq-style adapters (Faircloth and Glenn 2012). They were pooled after random shearing and individual barcoding and sequenced in a single lane of an Illumina HiSeq platform. The eighth genome was

193 sequenced at a higher coverage by means of two 101-bp paired-end shotgun libraries
194 and two 101-bp mate-paired libraries with insert sizes of 8 Kb in length at Macrogen
195 Inc. The TruSeq Nano DNA Kit (Illumina) was used for the preparation of the shotgun
196 libraries, while the mate-paired libraries were prepared with Nextera Mate Pair Kit
197 (Illumina). We used FASTQC (Andrews 2010) to evaluate the quality of the sequenced
198 data, and quality filtering was carried out with NextClip (Leggett et al. 2013) in the case
199 of the mate paired libraries. For the rest of them we used Trimmomatic (Bolger et al.
200 2014), applying a sliding window filtering approach with a size of 4 bp and a phred
201 quality score threshold of 25. We also set a minimum length of 50 bp, below which
202 reads were filtered out after trimming. We used the software SOAPDENOVO2 (Luo et
203 al. 2012) to perform the assembly. The average insert size for each library was
204 estimated in a preliminary run, and we set a Kmer size of 27 and minimum edge
205 coverage of 2. Gaps that emerged during the scaffolding process were removed with the
206 GapCloser tool from SOAPDENOVO2. Finally, we filtered out all the scaffolds shorter
207 than 500 bp so the genome was functional as a mapping reference. The final assembled
208 genome had 37,904 scaffolds with an N50 of 147,816 bases, a L50 of 1,951 scaffolds, a
209 total size of 1.09 Gb, 17.5 Mb of missing sites, and an overall coverage of ~56X, as
210 computed with VCFTOOLS version 0.1.13 (Danecek et al. 2011).
211
212 *Genotyping-by-sequencing*
213 We used genotyping-by-sequencing (Elshire *et al.* 2011) to obtain individual genotypes
214 from 127 Oregon juncos belonging to the following subspecific taxa: *townsendi* (n=16),
215 *pontilis* (n=16), *thurberi* (n=35), *pinosus* (n=16), *montanus* (n=16), *shufeldti* (n=12),
216 *oreganus* (n=16) (Table 1). GBS libraries were prepared and sequenced at Cornell
217 University's Institute for Genomic Diversity, using the restriction enzyme PstI for

digestion. Sequencing of the 127 individually-barcoded libraries was carried out in three different lanes (along with other 149 junco samples intended for other studies) of an Illumina HiSeq 2000, resulting in an average of 229.2 million good single-end reads 100 bp in length per lane. Samples of the same form were distributed among at least two of the lanes to avoid sequencing bias, except in the case of *shufeldti* individuals, which were all introduced in the last set of sequenced samples.

Alignment and variant calling

We evaluated GBS read quality using FASTQC after sorting them by individual with FASTXTOOLKIT (Gordon and Hannon 2010), and performed the trimming and filtering treatment using PRINSEQ (Schmieder and Edwards 2011). All resulting reads were 69 bp long and had a mean genotyping phred quality score of at least 30, with no positions below 20. The reads were then mapped against the assembled junco genome using the mem algorithm in the Burrows-Wheeler Aligner (BWA, Li and Durbin 2009). Two samples were excluded at this step due to too low read mapping (1 *thurberi* and 1 *montanus*). We used the Genome Analysis Toolkit (GATK, McKenna et al. 2010) version 3.6-0 to realign reads around indels using the IndelRealigner tool and then we applied the HaplotypeCaller tool to call the individual genotypes. We finally used the GenotypeGVCFs tool to gather all the per-sample GVCFs files generated in the previous step and produce a set of joint-called SNPs and indels in the variant call format (*vcf*) (GATK Best Practices, DePristo et al. 2011; Auwera et al. 2013). Because GBS data do not provide enough coverage for base quality score recalibration, we used VCFTOOLS to implement a 'hard filtering' process, customized for each of the downstream analyses (Table 2).

Genetic structure analyses

To explore genome-wide population structure among all Oregon junco forms, we ran a principal components analysis (PCA) based on SNP data. Using VCFTOOLS we retained all samples with less than 25% missing data after a 'soft filtering' (coverage range between 2 and 100, minimum phred quality score of 40), resulting in a dataset of 88 samples, and between 8 and 12 individuals per population (24 in the case of *thurberi*). We filtered out all the sites with any non-genotyped individuals or a minor allele frequency (MAF) below 0.02. We also applied a threshold for SNPs showing highly significant deviations from Hardy-Weinberg equilibrium (HWE) with a p-value of 10^{-4} to filter out false variants arisen by the alignment of paralogous loci, resulting in a matrix of 11,261 variants. We then excluded SNPs putatively under selection using BayeScan (Foll and Gaggiotti 2008). BayeScan computes per-SNP F_{ST} scores and decomposes them into a population-specific component shared by all loci that approximates population related effects, and a locus-specific component shared by all populations, which accounts for selection. The program compares two models of divergence, with and without selection, and assumes a departure from neutrality when the locus-specific component is necessary to explain a given diversity pattern (Foll 2012). We used BayeScan with default settings and a thinning interval size to 100 to ensure convergence. For each SNP we obtained the posterior probability for the selection model and the F_{ST} coefficient averaged over populations. For outlier detection and exclusion, we implemented a false discovery rate of 0.3. To filter out the SNPs under linkage disequilibrium (LD) we used the function snpgdsLDpruning from the SNPrelate package (Zheng 2012) in R Studio (R Studio Team 2015) version 1.0.136 with R (R Core Team 2013) version 3.2.2. We applied the correlation coefficient method with a threshold of 0.2 (method ="corr", ld.threshold=0.2), resulting in a final

data matrix of 9,436 SNP loci (Table 2). We then used the function snpgdsPCA also available in SNPrelate to perform the PCA and obtain the eigenvectors to be plotted.

We examined population structure with STRUCTURE (Pritchard et al. 2000), using a smaller, more heavily filtered SNP data matrix to reduce the computational time of the analysis. Using VCFTOOLS, we retained the eight samples of each population (16 in the case of *thurberi*) with the lowest proportion of missing sites for a final number of 64 samples. We constructed a data matrix of biallelic SNPs excluding those out of a range of coverage between 2 and 100, or with a genotyping phred quality score below 70. Positions with less than 90% of individuals genotyped were removed from the data matrix, along with those presenting a MAF below 0.02. Once again, we implemented a threshold for SNPs showing highly significant deviations from Hardy-Weinberg equilibrium (HWE) with a p-value of 10^{-4}, and performed the filtering for non-neutral positions and linkage disequilibrium exactly as done for the PCA, to obtain a final data matrix of 34,367 SNP loci (Table 2). We converted the *vcf* file to STRUCTURE format using PGDspider (Lischer and Excoffier 2012) version 2.0.5.1. Bash scripts to perform the analyses were created with STRAUTO (Chhatre and Emerson 2016) and we ran the program five times per K, with K ranging from 1 to 10 after running a preliminary analysis to infer the lambda value. The burn-in was set to 50K iterations and the analysis ran for an additional 100K iterations. Similarity scores among runs and graphics were computed with CLUMPAK (Kopelman et al. 2015).

Redundancy analysis and variance partition

When applying GEA methods there are two main potentially confounding effects related to neutral factors: (i) structure among populations derived from strong drift in

293 isolation may result in genetic patterns similar to those related to adaptive divergence;
294 and (ii) demographic expansions along latitudinal axes may create gradients of allele
295 frequencies at neutral loci correlated with latitude, that in turn would correlate with any
296 environmental variable that changes with latitude, mimicking a pattern of selective
297 sweep and local adaptation (Excoffier and Ray 2008; Excoffier et al. 2009; Rellstab et
298 al. 2015; Forester et al. 2016). Redundancy analysis (Van Den Wollenberg 1977;
299 Legendre and Legendre 1998) is a canonical ordination method that allows computing
300 the variance of a set of response variables explained by a number of constraining or
301 explanatory variables. In addition, partial RDA enables computation of this shared
302 variance between two sets of variables while conditioning or holding constant the
303 effects of a third set of covariables. Here we used RDA and partial RDA as
304 implemented in the R package vegan (Oksanen et al. 2016) to explore the associations
305 between genetic variability and environmental data. Ecological data were obtained from
306 7 of the 19 variables available in the BioClim database (Hijmans et al. 2005),
307 specifically chosen in accordance to their relevance to junco ecology (Miller 1941;
308 Nolan et al. 2002). They measured mean temperature and precipitation over the year
309 (BIO1 and BIO12); mean temperature and precipitation over the warmest quarter
310 (BIO10 and BIO18), which corresponds to the birds' breeding season; isothermality,
311 referring to how the range of day-to-night temperature differs from the range of
312 summer-to-winter, where a value of 100 indicates equality between them; and
313 seasonality of temperature and precipitation (BIO4 and BIO15). We also included three
314 vegetation variables from the Moderate Resolution Imaging Spectroradiometer
315 (MODIS) satellites as available in https://modis.gsfc.nasa.gov: percent tree cover
316 (TREE), Normalized Difference Vegetation Index (NDVI, a measure of canopy
317 greenness), and NDVI's annual standard deviation (std_NDVI). Finally, we included

318 the high-quality elevation data provided by the NASA Shuttle Radar Topographic
319 Mission (ELEV), downloadable from http://www2.jpl.nasa.gov/srtm for a total of
320 eleven variables (Table 3). All ecological variables were centered and standardized.
321 Following Blanchet et al. (2008), we implemented a forward selection method using the
322 forward.sel function from the R-package packfor (Dray et al. 2009) to reduce the
323 number of variables in the model. This procedure applies two stopping criteria: a
324 significance level for each tested variable, which we set at 0.01; and a maximum limit
325 for global adjusted R^2, equal to the adjusted R^2 of the RDA model including all initial
326 variables. In doing so we prevent inflation of the overall type I error and of the amount
327 of explained variance. After this, we excluded those retained variables with a variance
328 inflation factor (VIF) over 10 (Borcard et al. 2011) to avoid high collinearity. Despite
329 signs of low orthogonality observable among variables in the partial RDA (especially
330 among BIO18, TREE and NDVI, see Results) we chose not to exclude more variables
331 or to apply dimension-reduction treatments like PCA to the environmental space of
332 variables so as to assess their specific and relative contributions to differentiation
333 patterns (McCormack et al. 2010) and discuss signals of adaptation with higher
334 confidence. The final selected ecological variables were used as explanatory variables in
335 two RDAs, with and without subtracting the effects of neutral processes, which were
336 approximated by the first two principal components of the PCA of population structure
337 based on selectively neutral loci (see above). As response variables, we used the same
338 SNP dataset used for the PCA, but excluding LD and neutrality filters. SNP data were
339 coded as counts of the alternative allele for each position (*i.e.*, 0, 1 or 2 copies) with
340 VCFTOOLS and transformed following Patterson et al. (2006). Statistical significance
341 was obtained using a permutation-based procedure with 10,000 permutations, assuming
342 $\alpha = 0.01$. We also used variance partitioning as implemented in the vegan R-package to

343 estimate (i) the total proportion of genomic variation explained by ecological variables
344 alone; (ii) by neutral structure alone; and (iii) the effects of both sets of variables.
345 Finally, we repeated the whole RDA treatment for a subset of 87 SNPs identified as
346 selectively divergent by BayeScan, with no conditional treatment. The analyses were
347 conducted in R version 3.2.2 (code included in Appendix I, Supplementary Material).
348
349 *Niche divergence tests*
350 To further explore patterns of ecological divergence in the Oregon Junco, we tested for
351 niche divergence applying the method developed by McCormack et al. (2010), a method
352 that allows us to examine each environmental variable separately. To avoid a loss of
353 statistical power due to multiple analyses, we conducted three specific comparisons of
354 forms presenting different patterns of genetic divergence and geographical settings,
355 including: (i) *townsendi* and southern *thurberi* forms, in order to estimate niche
356 divergence between geographically isolated, genetically differentiated forms; (ii) the
357 ecologically divergent *pinosus* with the parapatric northern *thurberi* form, to further test
358 a possible case of isolation-by-adaptation; and (iii) northern and southern populations of
359 *thurberi*, as conspecific extremes of a potential adaptive gradient. We used occurrence
360 points from our own georreferenced field sampling records, and this set of occurrence
361 records was further revised to avoid spatial autocorrelation and to match the spatial
362 resolution of environmental variables (1-km grid). Our final dataset comprised 80
363 localities: *pinosus* (n = 14), *thurberi* north (n = 26), *thurberi* south (n = 19), and
364 *townsendi* (n = 21). We decided to improve quality (geographic accuracy) vs. quantity
365 (number of occurrence records), by using fewer data but with higher spatial accuracy
366 (Engler et al. 2004). To generate a background dataset for each population, we drew
367 1000 random points from a background representing the geographic range of each junco

368 population. In order to select an appropriately sized area for the niche divergence tests,
369 we included accessible habitats according to the dispersal ability of each population
370 (Soberon and Peterson 2005). We generated background samples from a 100-km
371 "buffer zone" around known occurrences (Warren et al. 2008). For populations with
372 small ranges or small dispersal ability (*thurberi* south, *pontilis* and *townsendi*) we
373 restricted the buffer zone to 10 km to reduce spatial inaccuracies in the null distribution
374 (Barve et al. 2011), after testing different buffer sizes to test the robustness in delimiting
375 accessible areas for juncos. Next, we extracted the environmental data (same as the data
376 used for the RDA, see above) for both occurrence points and random background points
377 from within the geographic range of each junco form. Niche divergence and
378 conservatism were tested by comparing the observed environmental differences among
379 forms against a null model of background divergence (generated by calculating the
380 difference between background points using a bootstrapping approach and 1000
381 resamples) for each environmental variable using a two-tailed test. We conducted all the
382 analyses in R 3.2.2.
383
384 *Genome scans*
385 We performed genome scans for different Oregon junco forms using BayeScan.
386 In order to obtain the chromosomic positions of the SNPs, we mapped the GBS reads
387 against the zebra finch (*Taeniopygia guttata*) genome v87 available in Ensembl (Yates
388 et al. 2016), applying the same set of tools and parameters as for mapping against the
389 junco genome. Using the same set of samples as in the PCA and the RDA, we
390 conducted the analysis for all forms together; for *townsendi* against *pontilis*; and for
391 *townsendi* against all *thurberi* (see Table 2 for final dataset sizes). For each of these
392 matrices, we retained only biallelic SNPs with coverage between 2 and 100 and a

393 genotyping phred quality score over 40. Positions with less than 25% of the individuals
394 genotyped were removed from each data matrix, along with those presenting a MAF
395 below 0.05. Once again, we implemented a p-value threshold for HWE of 10^{-4} to filter
396 out false variants arisen by the alignment of paralogous loci. We ran BayeScan with the
397 same settings used for filtering out SNPs under selection in population structure
398 analyses, but implemented a more conservative 10% FDR for outlier detection. Genome
399 scan plots were conducted in R 3.2.2 using the package qqman (Turner 2014).
400
401
402 **Results**
403
404 *Neutral genetic structure*
405 The plot of the first two principal components from the PCA revealed four distinct
406 clusters in the Oregon junco group. The most differentiated groups were *townsendi* and
407 *pontilis* from Baja California, which formed two highly divergent clusters with respect
408 to each other and to other populations. A third, highly differentiated group corresponded
409 to *pinosus* from coastal California, showing less differentiation than the Baja California
410 forms with respect to a fourth cluster, which included all the remaining forms in the
411 PCA (Fig. 1B). Within this fourth cluster, southern *thurberi* individuals presented
412 certain degree of differentiation from the rest of the forms, a pattern more conspicuous
413 when plotting the third and fourth components, which also revealed a slight signal of
414 divergence in the *oreganus* form (Fig. S1 in Supplementary Information).
415
416 The STRUCTURE results were generally congruent with the PCA. The K = 2 plot
417 recovered *townsendi* as an independent population, which shared a considerable amount

418 of variance with *pontilis*. In the analysis for K = 3, *pontilis* separated, and K = 4
419 identified the same four main clusters seen in the PC1 vs. PC2 plot (Fig. 1B), revealing
420 *pinosus* as an independent genetic cluster. The plot for K = 5 clearly captured the
421 differentiation of the southern *thurberi* form in a fifth cluster, and in K=6, *oreganus*
422 appears as an independent northern group with all individuals from northern *thurberi*
423 and especially *montanus* and *shufeldti* forms showing an increasing probability of
424 assignment to the *oreganus* cluster from south to north (Fig. 2).
425
426 Patterns of divergence in Nei's distances and F_{ST} values among forms were highly
427 congruent with previous results, with *townsendi*, *pontilis* and *pinosus* showing the
428 highest values for both indices, and northern forms showing lower levels of
429 differentiation, especially between southern and northern *thurberi* individuals (Table
430 S1).
431
432 *Forward selection of explanatory variables*
433 Out of eleven potentially relevant ecological variables for juncos, six were retained after
434 the forward selection method intended for excluding non-significant effects. Retained
435 variables included isothermality (BIO3), mean temperature of the warmest quarter
436 (BIO10), mean precipitation of the warmest quarter (BIO18), vegetation cover (TREE),
437 greenness (NDVI), and elevation (ELEV) (Table 3). None of these variables was
438 excluded due to excessive correlation as VIF values were below 10 (maximum
439 recovered VIF = 5.75).
440
441 *Redundancy analysis and variance partition*

All six ecological variables retained in the forward selection method were included as explanatory variables in the RDA and the partial RDA models. RDA computes, in successive order, a series of axes that are linear combinations of the explanatory variables, and that best explain the variation in the matrix of response variables (Borcard et al. 2011). Six RDA axes (named RDA1 to RDA6 hereafter, ordered by the amount of variance explained by each one, as reflected by the adjusted R^2) explained 6.26% of the total genetic variance in the non-conditioned model, and 1.18% when removing the effects of neutral genetic structure (Table 4). The amount of explained variance increased to 36.61% when using only BayeScan outliers as response variables (Table 4, Table S2). The permutation tests for the RDA models yielded a p-value below 0.001 in all three analyses, confirming the significance of the constraining variable effects.

Loadings of ecological explanatory variables on each of the axes varied across the three different RDA models (Fig 4, Table 4, Table S2). In the non-conditioned RDA, the RDA1 axis had a large negative contribution of TREE and NDVI, and loaded positively on elevation (Fig. 4A). The RDA2 axis loaded mostly on BIO3 and BIO10. The plot of per-individual projections on these two axes revealed a pattern generally similar to the PCA. The forms *townsendi*, *pontilis* and to a lesser extent *pinosus*, showed distinctive high values of correlation with both axes. The remaining forms showed similar correlation patterns with respect to RDA1, with southern *thurberi* individuals showing a clear association with RDA2 (Fig. 4A).

In the partial RDA, RDA1 had a large contribution of BIO3, while RDA2 loaded mostly on BIO10 and to a lesser extent, BIO18 and TREE (Fig. 4B). Plotting these first two

RDA axes revealed patterns of genetic correlation especially related to the first RDA axis for *pinosus*, which consequently presented the strongest association with isothermality. The individuals from the southern population of *thurberi* showed a more pronounced negative association with RDA2 than in the non-conditioned RDA, further evidence of a positive correlation with mean temperature of the warmest quarter. Northern forms of the Oregon junco (northern *thurberi*, *shufeldti*, *montanus* and *oreganus*) also separated along the second RDA axis, with the northernmost *oreganus* showing the strongest association with the particularly conspicuous mean precipitation of the warmest quarter gradient, a pattern that was not visible in the non-conditioned RDA. *Townsendi* from Baja California occupied positions closer to the origin of coordinates, suggesting a lower association between environmental and genetic variance (Fig. 4B).

In the RDA based on outlier loci potentially under selection, the first axis showed moderate negative contributions from TREE and NDVI, and also a positive contribution of ELEV (Fig. 4C). Variance in BIO18 was almost entirely captured by RDA2, which also had a relatively high, negative contribution from BIO3. The plot showed a pattern of correlation between *pontilis* and *townsendi* along RDA1, while genetic variance in *oreganus* appeared strongly associated with the gradient of mean precipitation of the warmest quarter along RDA2. The rest of Oregon junco forms (and one atypical *oreganus* individual) were distributed in an opposite fashion, with small differences in their patterns of correlation with environmental variability captured in the second axis of the RDA (Fig. 4C).

The variance partition analysis showed that climate and neutral structure together explained 7.17% of the total genetic variability (fractions A+B+C, Fig. 5). Since variable sets are not orthogonal, a 5.08% of variation was explained jointly by the environmental data and the first two components of the PCA based on neutral genetic positions (fraction B, Fig. 5). As recovered in the partial RDA, environmental variables alone explained 1.18% of the total variance (fraction A, Fig. 5), while the non-overlapping fraction of neutral genetic structure explained 0.91% of the variability in the SNP dataset (fraction C, Fig. 5). The p-value computed through the 10,000-step permutation test for each individual fraction was below 0.001 in all cases, thus confirming the significant effects of both variable sets.

Niche divergence tests

We tested for niche divergence and conservatism on each of the environmental variables. We found significant niche divergence between *pinosus* and northern *thurberi* for three of the six environmental variables analyzed (isothermality, mean precipitation of the warmest quarter and elevation; Table 5). When considering northern *thurberi* vs. southern *thurberi*, we found significant divergence for mean temperature of the warmest quarter and conservatism for isothermality (Table 5). NDVI was the only variable that exhibited significant divergence between *townsendi* and *thurberi* south (Table 5).

Genome scans

The BayeScan survey comparing all Oregon junco forms together detected 32 SNPs potentially under divergent selection, and 5 significant SNPs potentially under balancing selection. In the two pairwise comparisons *townsendi* vs. *pontilis* and *townsendi* vs. *thurberi*, 20 and 30 significant SNPs with signs of having diverged under

selection were detected, respectively, and no significant SNPs under balancing selection were found in either case. SNPs potentially differentiated under divergent selection appeared distributed across the genome in all comparisons, without obvious signs of heterogeneity among regions (Fig. 6). Chromosomes 1B and 16 harbored no SNPs so they are not shown in the plot.

Discussion

Neutral population structure and local adaptation explains genomic variance among Oregon junco forms

Our results reveal that both neutral and selective factors have played a role in driving divergence among Oregon junco populations, and that the relative contributions of geographic isolation and environment-driven selection are not uniform across the distribution range of the complex. Environmental variables explained 1.18% of genomic variation when controlling for population structure, and environment and neutral structure together accounted for 7.17% of the variability in the 11,256 SNP matrix. The remaining 92.83% of the variance corresponds potentially to loci under balancing selection or selective pressures not represented in our ecological variables, and to neutral variation shared by all Oregon junco forms because of their close relatedness and/or gene flow among them. The amount of variance explained solely by environmental variables in our study was comparable to the values reported in studies applying RDA to detect specific correlations between genomic variation and a given set of potentially correlated variables, as shown in plants (e.g. Lasky et al. 2012; Vincent et al. 2013; De Kort et al. 2014) or other avian species (Safran et al. 2016; Szulkin et al.

2016). Previous studies on birds have used simple spatial variables such as geographic distance to control for the effects of spatial autocorrelation (Safran et al. 2016; Szulkin et al. 2016). Here, we controlled for genome-wide patterns of neutral variation by subtracting the variance captured by the first two PCs of a PCA based on neutral genome-wide SNPs, a method which should better account for population history and structure, including changes in effective population size, geographic isolation and related effects (Forester et al. 2016). Since spatial autocorrelation is usually reflected by neutral genetic structure, we did not include spatial covariates to avoid over-conditioning the model (Rellstab et al. 2015). Given that only a small fraction of the surveyed genome is expected to be related to genes coding for climatic adaptation or linked to them (Meirmans 2015), a significant 1.18% of association between genomic variation and environmental variability in the conditioned (partial) RDA over only 11,261 genome-wide distributed SNPs is a compelling signal of local adaptation.

Genetic-environment association patterns in the diversification of the Oregon junco

The RDA revealed a number of strikingly different patterns of covariation between genetic variance and ecological variables likely to have played a role in Oregon junco diversification, especially when the effects of population history were removed. The forms *pontilis* and *townsendi* from Baja California, markedly isolated in terms of geography and neutral genetic variability, presented a low genetic-environment association when controlling for population history. This suggests that the differentiation between *townsendi* and *pontilis* is due largely to geographic isolation, in this case caused by unsuitable desert habitat in the lowlands surrounding their respective mountain ranges, a pattern also known as isolation by resistance (IBR, McRae and Beier 2007). In this scenario, our results suggest that differentiation is

566 caused by drift under conditions of small population size and reduced gene flow, rather
567 than divergent selection due to local adaptation, fitting the classic allopatric speciation
568 model (Mayr 1942, 1963; Coyne and Orr 2004). This hypothesis is consistent with the
569 niche divergence test comparing *townsendi* with southern *thurberi*, for which all tested
570 variables but NDVI showed no signal of divergence beyond expectations based on
571 background divergence.
572
573 The form *pinosus* showed considerable neutral genetic structure and a conspicuous
574 pattern of genetic-environment association in both non-conditioned and partial RDA.
575 When controlling for population structure, *pinosus* individuals showed high positive
576 correlation values with isothermality, while correlating negatively with elevation.
577 Indeed, *pinosus* presents the highest isothermality values, and the second lowest
578 elevation after *oreganus*, reflecting a tolerance for low elevation conditions that are
579 absent in neighboring *thurberi*, a pattern also recovered in the niche divergence test.
580 Unlike other differentiated forms like *pontilis* and *townsendi*, *pinosus* does not show
581 high geographic isolation, and zones of intergradation with *thurberi* have been
582 described (Miller 1941). Neutral population divergence despite the absence of
583 geographic barriers to gene flow along with signs of local adaptation is a pattern
584 consistent with isolation-by-adaptation, where barriers to gene flow may have arisen as
585 individuals adapted to the distinct habitat of the coastal mountains of California. Niche
586 distinctiveness and the genetic-environment association pattern of this form is thus
587 congruent with a combination of warm latitude, low elevation and coastal influence that
588 has seemingly resulted in the adaptive differentiation of *pinosus* from the rest of the
589 Oregon junco taxa. As a result, differentiation by drift may have led to positive
590 correlations between adaptive and neutral genetic divergence (Nosil et al. 2008).

591

592 The southern *thurberi* individuals from Mont Laguna showed high overlap in terms of
593 neutral genetic structure with northern *thurberi* and other boreal forms, and only slight
594 differences in their genetic-environment association patterns when no controls for
595 confounding factors were implemented. The Mount Laguna site represents the
596 southernmost tip of the *thurberi* range in Southern California, which extends northward
597 and reaches Oregon, forming a relatively continuous distribution (Miller 1941; Nolan et
598 al. 2002), suggesting potentially high gene flow. However, the partial RDA revealed a
599 distinctive pattern of high correlation with the mean temperature of the warmest quarter
600 for the southern *thurberi* juncos, differentiating them from the rest of Oregon forms.
601 They also correlated negatively with the mean precipitation of the warmest quarter. This
602 pattern seems congruent with the habitat of Mount Laguna, and in general with the
603 southern inland range of Oregon juncos, quite arid during summer but subject to
604 snowfalls in winter due to the high elevations (Miller 1941), contrasting sharply with
605 the more climatically moderate coastal and northern populations. The limited neutral
606 genetic structure between *thurberi* range extremes but considerable differentiation in the
607 genetic-environment association patterns is consistent with a process of local adaptation
608 across a selective gradient (Forester et al. 2016), in which selection is the prominent
609 evolutionary force driving differentiation (Haldane 1948; Slatkin 1973; Nagylaki 1975;
610 Felsenstein 1976) while neutral alleles may move freely across space. The niche
611 divergence test comparing southern and northern *thurberi* populations was significant
612 for mean temperature of the warmest quarter.

613

614 The boreal Oregon junco forms including *oreganus*, *montanus*, *shufeldti*, and *thurberi*
615 individuals from Tahoe, California, presented a more conspicuous pattern of local

616 adaptation along a shallow selective gradient. These forms showed very low neutral
617 genetic structure or differences in ecological covariances in the non-conditioned RDA,
618 yet showed an increasing signal of association following their latitudinal distribution in
619 the partial RDA. A strong association pattern emerged especially for mean precipitation
620 of the warmest quarter and for correlated environmental variables of tree cover and
621 greenness, matching quite precisely their latitudinal distribution along a gradient of
622 increasing humidity and vegetation cover. The ecology-related differences in genetic
623 variance, consistent with the taxonomic classification of these forms, is especially
624 relevant considering the relative phenotypic similarity of these taxa, and their apparent
625 intergradation (Miller 1941; Nolan et al. 2002).
626
627 GEA methods present a number of limitations, including potentially high rates of type I
628 error (see Supplementary Materials for details). Here, rather than detecting specific loci
629 under selection, we aimed to explore how selection and neutral processes shape the
630 variability in Oregon juncos, but the risk of finding false significant associations
631 between genetic variance and ecological parameters persists. To further test the
632 environmental associations revealed in this study, we implemented a highly
633 conservative approach using only BayeScan outliers as response variables in the model.
634 The non-conditioned RDA based on 87 SNP loci identified by BayeScan as potential
635 targets of divergent selection yielded relatively lower resolution than the partial RDA.
636 BayeScan has been shown to produce relatively few false positives, but it is also a
637 conservative approach, the sensitivity of which decreases with selection strength
638 (Narum and Hess 2011). The RDA suggests that BayeScan correctly identified outliers
639 related to low temperatures and high precipitation for *oreganus* samples, a pattern
640 congruent with the habitat and with the outcomes of previous analyses for this form. It

641 also detected highly differentiated positions in *pontilis* and *townsendi* that correlate with
642 RDA1, but in this case associations with specific environmental variables were lower,
643 and the pattern disappears in the RDA based on the entire SNP dataset when correcting
644 for population structure. This may suggest that BayeScan failed to exclude the effects of
645 demographic history, or in turn, that controlling for the genetic variance captured by the
646 PCA was overly conservative. BayeScan was also less successful in detecting adaptive
647 divergence in *pinosus*, and especially in northern Oregon junco forms, where selection
648 may be weaker or have acted during a shorter period. Nevertheless, the outlier SNP
649 dataset explained 36.61% of the total climatic variability, a considerable amount
650 compared with the full SNP data RDA models, indicating a good fit of the retained
651 outliers to the linear regression on the environmental parameters.
652
653 *Interactions among environment, geography and demographic processes result in three*
654 *different modes of divergence within the Oregon junco lineage*
655 The Oregon junco is one of the six phenotypically and genetically differentiated dark-
656 eyed junco taxa evolved during a northward expansion from Central America after the
657 last glacial maximum, c.a. 18,000 years ago (Milá et al. 2007; Friis et al. 2016). Similar
658 postglacial expansions have been reported for many other bird species (Seutin et al.
659 1995; Milá et al. 2000; 2006; Hansson et al. 2008; Malpica and Ornelas 2014; Alvarez
660 et al. 2015). However, the population structure documented in this study reveals a
661 variety of different spatial, selective and demographic factors not previously
662 documented in other avian taxa. In light of our genetic-environment association
663 analyses, the patterns recovered by the PCA and STRUCTURE analysis reveal at least
664 three different effects of geography and demographic history interacting to varying
665 degrees with selection in the process of Oregon junco diversification. First, the IBR

pattern of differentiation presented by *pontilis* and *townsendi* may suggest that these forms are peripheral remnants of an original, broader distribution of the Oregon juncos, thereafter isolated in 'sky islands' of Baja California and diverging predominantly by drift. Indeed, in his thorough monograph on the geographic variation in juncos, Alden Miller (1941) had perceptively suggested early on that the habitat of Oregon juncos from Baja California did not seem to account for their phenotypic differentiation from Californian forms, and that their distinctive traits appeared to be predominantly "historical" (p. 306). The spatial configuration and recovered patterns of neutral and adaptive divergence for *pontilis* and *townsendi* fit the first model of neutral divergence of isolated population in approximately similar habitats (scenario A in Fig. 2). Second, the IBA pattern found in *pinosus* suggests that the current area of intergradation corresponds to a secondary contact zone that formed after diverging in relative isolation, maybe linked to the ancient coastal closed-cone pine forest that has allegedly diminished since the Pleistocene (Miller 1941). The mode of divergence between parapatric populations in different habitats (scenario B in Fig. 2) has been only partially fulfilled, since local adaptation seems to have resulted in reduced levels of gene flow, leading to increased neutral genome-wide differentiation (Nosil et al. 2008; Funk et al. 2011; Flaxman et al. 2014). Third, the geographic continuum represented by *thurberi*, *shufeldti*, *montanus* and *oreganus* is also captured in the STRUCTURE analysis by a gradual signal of differentiation following a latitudinal distribution, suggesting that ongoing gene flow may occur among forms. Combined with the signal of increasing environmental association recovered in the partial RDA, these outcomes are consistent with a process of differentiation driven by local adaptation along a selective gradient in the direction of the northward expansion, fulfilling the third hypothesized mode of divergence for these forms of Oregon junco (scenario C in Fig. 2). Interestingly,

691 ecological association approaches have been shown to perform better along clines of
692 selection where demographic expansions align with the gradient of ecological variables,
693 usually related to latitude (Frichot et al. 2015), as is the case in the *Junco* system.
694
695 A relevant aspect of the marked population structure found among Oregon junco forms
696 is that it is based on a relatively small subset of genome-wide SNPs randomly sampled
697 from across the genome, representing a genomic fraction not greater than 0.2% of the
698 total of 1.2 Gb. The clear signal of divergence mediated by environmental factors
699 recovered also in the RDA indicates that divergence may have taken place at the level
700 of the entire genome, suggesting the role of multiple selective pressures during local
701 adaptation along the latitudinally broad and heterogeneous distribution of the Oregon
702 juncos. The presence of outliers potentially under positive selection scattered across the
703 genome seems to support this hypothesis of selection-driven genome-wide divergence,
704 rather than widespread drift among isolated populations. Other examples of such
705 patterns of genomic differentiation due to divergent selection at early (e.g. Parchman et
706 al. 2013; Brawand et al. 2014; Egan et al. 2015) and intermediate (e.g. Riesch et al.
707 2017) stages of speciation have been reported recently, contrasting with proposed
708 models of speciation initiated by divergent selection in a few, localized genes involved
709 in reproductive isolation (e.g. Nadeau et al. 2012; Poelstra et al. 2014).
710
711
712 **Conclusion**
713 Our analyses reveal the role of both local adaptation and demography in driving rapid
714 diversification during the northward recolonization of western North America by the
715 Oregon junco. The combined effects of a demographic expansion along a selective

716 gradient with a heterogeneous landscape of environmental variability have resulted in a
717 striking array of divergence modes within a single lineage, from isolated forms in Baja
718 California that have differentiated largely by drift in isolated 'sky islands', to adaptive
719 diversification along selective gradients with no obvious geographic barriers to gene
720 flow. There is also a compelling example of isolation by adaptation in the case of
721 *pinosus*, where ecological barriers to gene flow seem to maintain its divergence with
722 respect to nearby forms. Genome-wide patterns of divergence indicate that Oregon
723 junco diversification has been driven by multiple ecological factors acting on many loci
724 across the genome, and suggests that selection may promote local adaptation in short
725 periods of time, highlighting the role of adaptive divergence in the early stages of the
726 speciation process. Future analyses of dense sequencing and functional gene
727 characterization will be necessary to further identify adaptive changes promoting
728 barriers to gene flow and reveal the genomic architecture of rapid diversification.
729
730
731 **Acknowledgements**
732 We thank Pau Aleixandre, Jonathan Atwell, Elena Berg, Setefilla Buenavista, Steve
733 Burns, Jatziri Calderón, Adrián Gutiérrez, Alfonsina Hernández, Fritz Hertel, Ellen
734 Ketterson, Adán Oliveras de Ita, César Ríos, Sahid Robles, Vicente Rodríguez, Whitney
735 Tsai, Rich Van Buskirk and Alvar Veiga for invaluable help in the field and lab. We are
736 also grateful to Yoann Anselmetti, Clémentine Francois, Rachel Johnston, Etienne
737 Kornobis, Benoit Nabholz, Sergio Nigenda, Jacqueline Robinson, Marjolaine Rouselle
738 and Robert K. Wayne for their assistance with bioinformatic analyses. We also thank
739 Laura Barrios and Luis M. Carrascal for reviewing the statistical analyses and providing

orientation. Funding was provided by grant CGL-2011-25866 from the Spanish Ministry of Science and Innovation to BM.

Data Accessibility

Genomic data will be deposited in Dryad in short.

Author Contributions

G. Friis and BM designed the study and carried out field sampling; G. Friis, JM, and BF generated and analyzed genomic data; G. Friis, G. Fandos and AZ generated and analyzed environmental data; G. Friis and BM wrote the manuscript with input from all co-authors.

753 **Table 1.** Oregon junco forms and number of genotyped individuals per locality. State
754 abbreviations are the following: British Columbia (BC) in Canada; Oregon (OR),
755 California (CA) in the USA; Baja California Norte (BCN) in Mexico.

756

Form	*State*	*Localities*	*Sequenced*
oreganus	BC	Banks Island, Porcher Island, Susan Island	16
shufeldti	OR	Willamette N.F.	12
montanus	OR	Wallowa N.F.	16
northern *thurberi*	CA	Tahoe	18
southern *thurberi*	CA	Mount Laguna	17
pinosus	CA	Santa Cruz Mountains	16
pontilis	BCN	Sierra Juárez	16
townsendi	BCN	Sierra San Pedro Mártir	16
Total			127

757

758

759 **Table 2.** SNP data matrices used in each analyses. General filters included a depth
760 range from 2 to 100 and a p-value for Hardy-Weinberg deviation of 10^{-4}.
761

Analysis	**Number of samples**	**Min. phred score**	**MAF threshold**	**Number of SNPs**	**Allowed missing data**
STRUCTURE	64	70	0.02	34,367	10%
PCA	88	40	0.02	9,436	0%
RDA:					
On all *loci*	88	40	0.02	11,261	0%
On BayeScan outliers	88	40	0.02	87	0%
Genome Scans:					
All lineages	88	40	0.02	29,868	75%
townsendi vs. *pontilis*	24	40	0.05	22,773	75%
townsendi vs. *thurberi*	24	40	0.05	22,516	75%

762
763

764 **Table 3.** Set of environmental variables included in the initial stepforward selection

765 method. Significant variables retained by the method are shown in bold.

766

Environmental variable	Description
BIO1	Annual mean temperature
BIO3	**Isothermality**
BIO4	Temperature seasonality (standard deviation *100)
BIO10	**Mean temperature of the warmest quarter**
BIO12	Annual precipitation
BIO15	Precipitation seasonality (coefficient of variation)
BIO18	**Precipitation of the warmest quarter**
NDVI	**Normalized Difference Vegetation Index (greenness)**
NDVI SD	Annual NDVI standard deviation (greenness seasonality)
TREE	**Percent tree cover**
ELEV	**Elevation from the NASA Shuttle Radar Topographic Mission**

767

768 **Table 4.** RDA loads of the constraining variables in the first two axes and their
769 explained variance for each one of the RDA models. The total variance explained by the
770 full model (adjusted R^2 for the resultant six axes) is shown for each analysis. In all of
771 the three analyses, the p-value for the full models was below 0.001. See Table 3 for
772 variable definitions.
773

	Non conditioned RDA		**Partial RDA**		**RDA of BayeScan outliers**	
Total explained variance (adjusted R^2)	6.26%		1.18%		36.61%	
Variable	RDA1	RDA2	RDA1	RDA2	RDA1	RDA2
BIO3	0.124	0.239	0.839	-0.427	0.214	0.763
BIO10	0.108	-0.610	0.359	-0.679	0.221	0.374
BIO18	0.052	0.021	-0.452	0.501	-0.031	-0.994
ELEV	0.646	-0.031	-0.324	-0.301	0.629	0.420
NDVI	-0.641	0.588	-0.320	0.199	-0.731	-0.277
TREE	-0.710	0.320	-0.270	0.326	-0.776	-0.423
Variance						
Eigenvalue	1304.262	567.705	481.320	350.714	63.655	12.657
Proportion explained	0.025	0.011	0.003	0.002	0.250	0.050
Cumulative proportion	0.025	0.037	0.003	0.005	0.250	0.300

774
775

776 **Table 5.** Results from the niche divergence test for *pinosus* vs. northern *thurberi*,
777 northern vs. southern *thurberi* and southern *thurberi* vs. *townsendi*. Variables showing
778 significant divergence (Diverged) or conservatism (Conserved) are shown in bold (p-
779 value < 0.05). e.d.b.b.: expected divergence based on background.

780

	Variable	Result	p-value	Observed mean difference	Background mean difference
pinosus vs.	TREE	e.d.b.b.	0.636	3.95	7.17
northern *thurberi*	BIO10	e.d.b.b.	0.718	20.40	17.34
	BIO3	**Diverged**	**0.000**	**16.78**	**9.45**
	BIO18	**Diverged**	**0.000**	**41.92**	**27.24**
	ELEV	**Diverged**	**0.032**	**1329.81**	**978.26**
	NDVI	e.d.b.b.	0.550	192.67	428.18
northern vs.	TREE	e.d.b.b.	0.580	2.11	4.52
southern *thurberi*	**BIO10**	**Diverged**	**0.030**	**41.85**	**23.87**
	BIO3	**Conserved**	**0.002**	**1.37**	**2.87**
	BIO18	e.d.b.b.	0.860	15.02	14.25
	ELEV	e.d.b.b.	0.474	202.60	140.29
	NDVI	e.d.b.b.	0.144	258.89	1019.97
southern *thurberi*	TREE	e.d.b.b.	0.536	15.01	12.25
vs. t*ownsendi*	BIO10	e.d.b.b.	0.412	47.88	43.03
	BIO3	e.d.b.b.	0.472	2.47	2.89
	BIO18	e.d.b.b.	0.188	74.77	67.26
	ELEV	e.d.b.b.	0.786	750.22	717.21
	NDVI	**Diverged**	**0.012**	**1597.62**	**574.28**

781

782

783

784 **Figure 1.** Geographic distribution and neutral genetic structure of the Oregon junco
785 forms. (A) Breeding ranges of all the Oregon junco forms. (B) Genetic structure of
786 Oregon junco forms based on a principal components analysis of independent,
787 selectively neutral genome-wide SNPs.

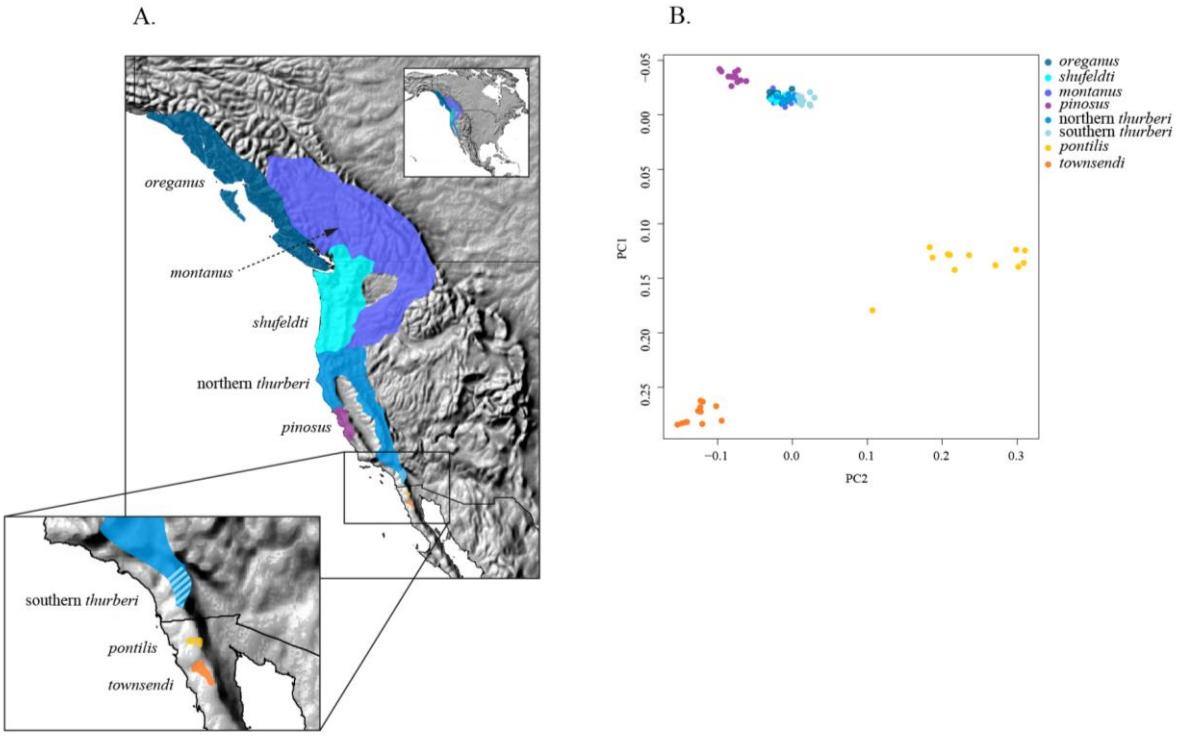

788

789

790

791 **Figure 2.** Expectations for neutral and adaptive divergence under different
792 environmental and spatial configurations found across the Oregon junco distribution.
793 (A) Geographically isolated populations in similar habitats. (B) Parapatric populations
794 in ecologically divergent habitats. (C) Population continuum across a selective gradient.

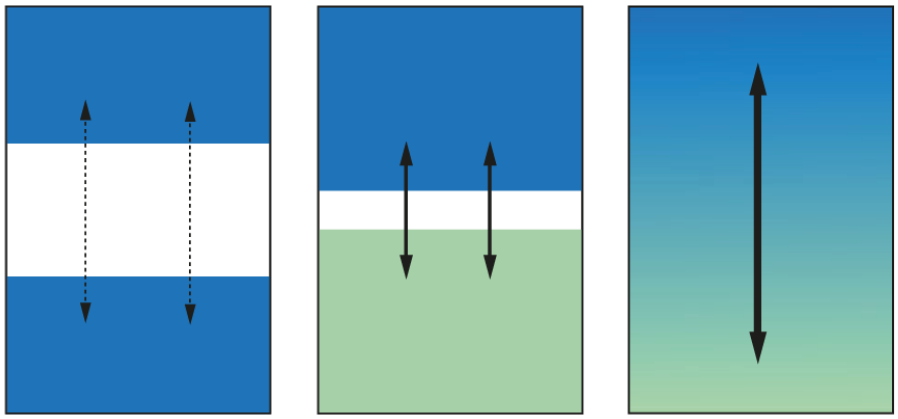

	A.	B.	C.
Habitat types:	ONE	TWO	GRADIENT
Gene flow:	LOW	MODERATE	HIGH
Neutral divergence:	HIGH	MODERATE	LOW
Adaptive divergence:	LOW	HIGH	HIGH

795

796

797 **Figure 3.** Genetic structure of the Oregon junco forms based on 34,367 selectively
798 neutral genome-wide SNPs using the program STRUCTURE. Each horizontal bar
799 corresponds to an individual, with colors corresponding to posterior assignment
800 probabilities to each of a number of genetic clusters (K). Colors correspond
801 approximately to those in Fig. 2A.
802

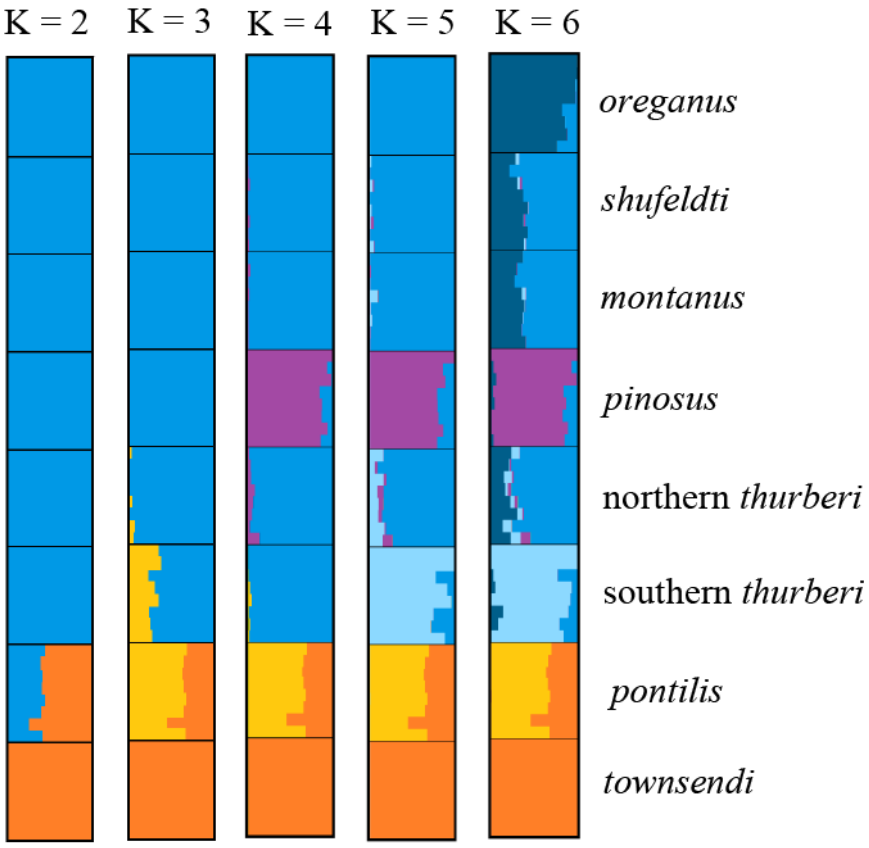

803
804
805

806 **Figure 4.** Genetic-environment association analyses in the Oregon junco. Points
807 represent the projection of individual genotypes on the first two RDA axes. Marker
808 colors correspond to those on the range map on Fig. 2A. The explanatory variables are
809 shown within the space defined by RDA1 and RDA2 by labeled vectors. Their
810 contribution to each axis is represented by the length of their orthogonal projections
811 over the scale bars along top and right sides of the graphs. Arrows indicate the direction
812 of the gradient of variation for the corresponding environmental parameter. The value
813 for each sample point on each explanatory variable can be obtained by an orthogonal
814 projection on the corresponding plotted vector. (A) First two RDA axes of a non-
815 conditioned RDA based on 11,261 SNPs. (B) First two RDA axes of a partial RDA
816 based on 11,261 SNPs conditioned by neutral genetic structure, approximated by the
817 first two PCs of a PCA based on neutral markers. (C) First two RDA axes of a non-
818 conditioned RDA based on 87 SNP outliers identified in a BayeScan analysis.

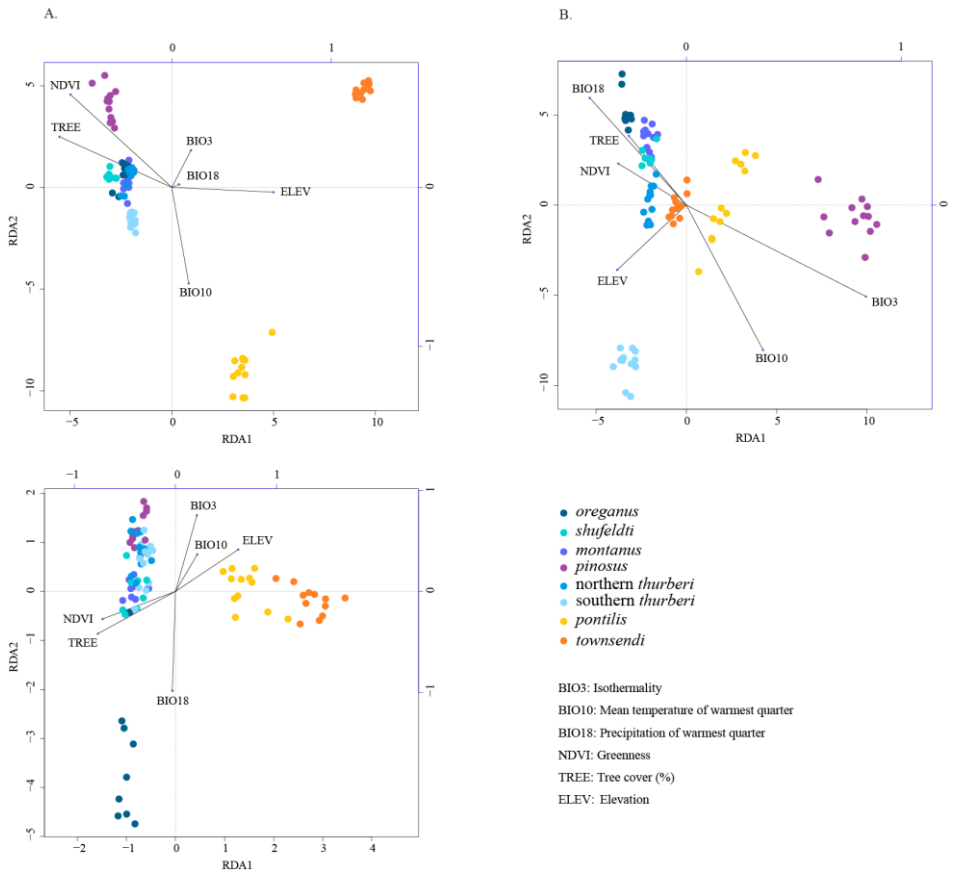

819

820 **Figure 5.** Plot of the fractions of the genetic variability in Oregon samples explained by
821 (A) environmental variables alone; (B) the overlap of both environmental variables and
822 neutral structure; and (C) neutral genetic structure alone; and the unexplained genetic
823 variability (residuals). P-values computed through a 1000-step permutation test for the
824 fractions A, B and C, were below 0.001 in all cases.
825

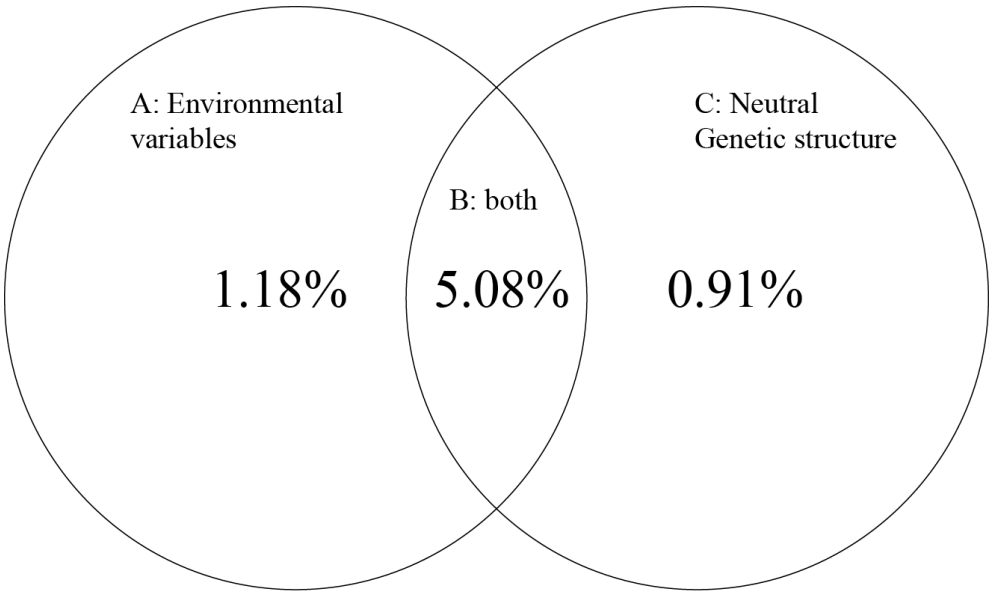

826
827

828 **Figure 6.** Plot of per-SNP posterior probability of divergence mediated by selection
829 (shown as 1 – Q-value as computed by BayeScan) in (A) all Oregon junco forms
830 together; (B) *townsendi* against *pontilis* and (C) *townsendi* against all *thurberi*. Loci
831 above the dotted line (in red) are those below a false discovery rate of 10%.
832

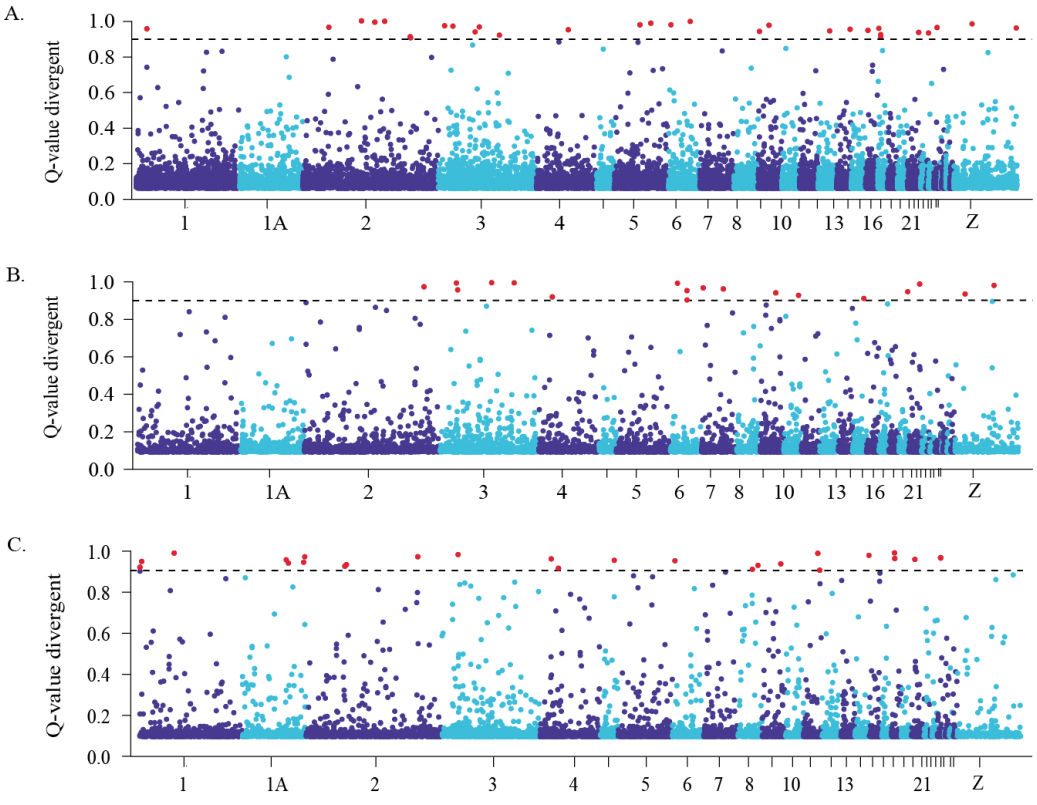

833
834

References

Alvarez, S., J. F. Salter, J. E. McCormack, and B. Milá. 2015. Speciation in mountain refugia: phylogeography and demographic history of the pine siskin and black-capped siskin complex. Journal of Avian Biology 47:335-345.

Andrews, S. 2010. FastQC: a quality control tool for high throughput sequence data.

Auwera, G. A., M. O. Carneiro, C. Hartl, R. Poplin, G. del Angel, A. Levy-Moonshine, T. Jordan, K. Shakir, D. Roazen, and J. Thibault. 2013. From FastQ data to high-confidence variant calls: the genome analysis toolkit best practices pipeline. Current protocols in bioinformatics:11.10. 11-11.10. 33.

Barve, N., V. Barve, A. Jiménez-Valverde, A. Lira-Noriega, S. P. Maher, A. T. Peterson, J. Soberón, and F. Villalobos. 2011. The crucial role of the accessible area in ecological niche modeling and species distribution modeling. Ecological Modelling 222:1810-1819.

Bierne, N., J. Welch, E. Loire, F. Bonhomme, and P. David. 2011. The coupling hypothesis: why genome scans may fail to map local adaptation genes. Molecular Ecology 20:2044-2072.

Billiard, S., T. Lenormand, and S. Gavrilets. 2005. Evolution of migration under kin selection and local adaptation. Evolution 59:13-23.

Blanchet, F. G., P. Legendre, and D. Borcard. 2008. Forward selection of explanatory variables. Ecology 89:2623-2632.

Bolger, A. M., M. Lohse, and B. Usadel. 2014. Trimmomatic: a flexible trimmer for Illumina sequence data. Bioinformatics:btu170.

Borcard, D., F. Gillet, and P. Legendre. 2011. Chapter 6. Canonical Ordination. Pp. 153-226. Numerical Ecology with R. Springer.

859 Brawand, D., C. E. Wagner, Y. I. Li, M. Malinsky, I. Keller, S. Fan, O. Simakov, A. Y.
860 Ng, Z. W. Lim, and E. Bezault. 2014. The genomic substrate for adaptive
861 radiation in African cichlid fish. Nature 513:375.
862 Carson, H. L. 1975. The genetics of speciation at the diploid level. The American
863 Naturalist 109:83-92.
864 Chhatre, V. and K. Emerson. 2016. StrAuto: Automation and parallelization of
865 STRUCTURE analysis. See http://strauto. popgen. org.
866 Christmas, M. J., E. Biffin, M. F. Breed, and A. J. Lowe. 2016. Finding needles in a
867 genomic haystack: targeted capture identifies clear signatures of selection in a
868 nonmodel plant species. Molecular Ecology 25:4216-4233.
869 Coyne, J. A. and H. A. Orr. 2004. Speciation. Sinauer Associates, Inc., Sunderland,
870 Massachusetts.
871 Danecek, P., A. Auton, G. Abecasis, C. A. Albers, E. Banks, M. A. DePristo, R. E.
872 Handsaker, G. Lunter, G. T. Marth, and S. T. Sherry. 2011. The variant call
873 format and VCFtools. Bioinformatics 27:2156-2158.
874 Darwin, C. 1859. The origin of species by means of natural selection, or the
875 preservation of favoured races in the struggle for life. John Murray, London.
876 De Kort, H., K. Vandepitte, H. H. Bruun, D. Closset-Kopp, O. Honnay, and J. Mergeay.
877 2014. Landscape genomics and a common garden trial reveal adaptive
878 differentiation to temperature across Europe in the tree species Alnus glutinosa.
879 Molecular ecology 23:4709-4721.
880 DePristo, M. A., E. Banks, R. Poplin, K. V. Garimella, J. R. Maguire, C. Hartl, A. A.
881 Philippakis, G. Del Angel, M. A. Rivas, and M. Hanna. 2011. A framework for
882 variation discovery and genotyping using next-generation DNA sequencing data.
883 Anglais 43:491-498.

884 Dray, S., P. Legendre, and G. Blanchet. 2009. packfor: Forward Selection with
885 permutation. R package version 0.0-7/r58.
886 Dwight, J. 1918. The geographical distribution of color and of other variable characters
887 in the genus *Junco*: a new aspect of specific and subspecific values. Bull. Am
888 Mus. Nat. Hist. 38:269-309.
889 Edmonds, C. A., A. S. Lillie, and L. L. Cavalli-Sforza. 2004. Mutations arising in the
890 wave front of an expanding population. Proceedings of the National Academy of
891 Sciences of the United States of America 101:975-979.
892 Egan, S. P., G. J. Ragland, L. Assour, T. H. Powell, G. R. Hood, S. Emrich, P. Nosil,
893 and J. L. Feder. 2015. Experimental evidence of genome-wide impact of
894 ecological selection during early stages of speciation-with-gene-flow. Ecology
895 letters 18:817-825.
896 Elshire, R. J., J. C. Glaubitz, Q. Sun, J. A. Poland, K. Kawamoto, E. S. Buckler, and S.
897 E. Mitchell. 2011. A Robust, Simple Genotyping-by-Sequencing (GBS)
898 Approach for High Diversity Species. PLoS ONE 6:e19379.
899 Engler, R., A. Guisan, and L. Rechsteiner. 2004. An improved approach for predicting
900 the distribution of rare and endangered species from occurrence and pseudo-
901 absence data. Journal of applied ecology 41:263-274.
902 Excoffier, L., T. Hofer, and M. Foll. 2009. Detecting loci under selection in a
903 hierarchically structured population. Heredity 103:285-298.
904 Excoffier, L. and N. Ray. 2008. Surfing during population expansions promotes genetic
905 revolutions and structuration. Trends in ecology & evolution 23:347-351.
906 Faircloth, B. C. and T. C. Glenn. 2012. Not all sequence tags are created equal:
907 designing and validating sequence identification tags robust to indels. PloS one
908 7:e42543.

909 Faria, R., S. Renaut, J. Galindo, C. Pinho, J. Melo-Ferreira, M. Melo, F. Jones, W.
910 Salzburger, D. Schluter, and R. Butlin. 2014. Advances in Ecological
911 Speciation: an integrative approach. Molecular ecology 23:513-521.
912 Felsenstein, J. 1976. The theoretical population genetics of variable selection and
913 migration. Annual review of genetics 10:253-280.
914 Flaxman, S. M., A. C. Wacholder, J. L. Feder, and P. Nosil. 2014. Theoretical models
915 of the influence of genomic architecture on the dynamics of speciation.
916 Molecular ecology 23:4074-4088.
917 Foll, M. 2012. Bayescan v2. 1 user manual. Ecology 20:1450-1462.
918 Foll, M. and O. E. Gaggiotti. 2008. A genome scan method to identify selected loci
919 appropriate for both dominant and codominant markers: A Bayesian perspective.
920 Genetics 180:977-993.
921 Forester, B. R., M. R. Jones, S. Joost, E. L. Landguth, and J. R. Lasky. 2016. Detecting
922 spatial genetic signatures of local adaptation in heterogeneous landscapes.
923 Molecular ecology 25:104-120.
924 Forester, B. R., J. R. Lasky, H. H. Wagner, and D. L. Urban. 2017. Comparing methods
925 for detecting multilocus adaptation with multivariate genotype-environment
926 associations. bioRxiv.
927 Frichot, E., S. D. Schoville, P. de Villemereuil, O. E. Gaggiotti, and O. François. 2015.
928 Detecting adaptive evolution based on association with ecological gradients:
929 orientation matters! Heredity 115:22-28.
930 Friis, G., P. Aleixandre, R. Rodríguez-Estrella, A. G. Navarro-Sigüenza, and B. Milá.
931 2016. Rapid postglacial diversification and long-term stasis within the songbird
932 genus Junco: phylogeographic and phylogenomic evidence. Molecular Ecology
933 25:6175-6195.

934 Funk, D. J., S. P. Egan, and P. Nosil. 2011. Isolation by adaptation in Neochlamisus leaf
935 beetles: host-related selection promotes neutral genomic divergence. Molecular
936 Ecology 20:4671-4682.
937 Gordon, A. and G. Hannon. 2010. Fastx-toolkit. FASTQ/A short-reads preprocessing
938 tools (unpublished) http://hannonlab. cshl. edu/fastx_toolkit.
939 Haldane, J. B. 1948. The theory of a cline. Journal of genetics 48:277-284.
940 Hansson, B., D. Hasselquist, M. Tarka, P. Zehtindjiev, and S. Bensch. 2008. Postglacial
941 colonisation patterns and the role of isolation and expansion in driving
942 diversification in a passerine bird. PLoS One 3:e2794.
943 Hedrick, P. W., M. E. Ginevan, and E. P. Ewing. 1976. Genetic polymorphism in
944 heterogeneous environments. Annual review of Ecology and Systematics 7:1-32.
945 Hijmans, R. J., S. E. Cameron, J. L. Parra, P. G. Jones, and A. Jarvis. 2005. Very high
946 resolution interpolated climate surfaces for global land areas. International
947 Journal of Climatology 25:1965-1978.
948 Jones, M. R., B. R. Forester, A. I. Teufel, R. V. Adams, D. N. Anstett, B. A. Goodrich,
949 E. L. Landguth, S. Joost, and S. Manel. 2013. Integrating landscape genomics
950 and spatially explicit approaches to detect loci under selection in clinal
951 populations. Evolution 67:3455-3468.
952 Kawecki, T. J. and D. Ebert. 2004. Conceptual issues in local adaptation. Ecology
953 letters 7:1225-1241.
954 Kopelman, N. M., J. Mayzel, M. Jakobsson, N. A. Rosenberg, and I. Mayrose. 2015.
955 Clumpak: a program for identifying clustering modes and packaging population
956 structure inferences across K. Molecular ecology resources 15:1179-1191.

957 Lasky, J. R., D. L. Des Marais, J. McKAY, J. H. Richards, T. E. Juenger, and T. H.
958 Keitt. 2012. Characterizing genomic variation of Arabidopsis thaliana: the roles
959 of geography and climate. Molecular Ecology 21:5512-5529.
960 Legendre, P. and L. Legendre. 1998. Numerical ecology: second English edition.
961 Developments in environmental modelling 20.
962 Leggett, R. M., B. J. Clavijo, L. Clissold, M. D. Clark, and M. Caccamo. 2013.
963 NextClip: an analysis and read preparation tool for Nextera Long Mate Pair
964 libraries. Bioinformatics:btt702.
965 Li, H. and R. Durbin. 2009. Fast and accurate short read alignment with Burrows–
966 Wheeler transform. Bioinformatics 25:1754-1760.
967 Lischer, H. E. L. and L. Excoffier. 2012. PGDSpider: an automated data conversion tool
968 for connecting population genetics and genomics programs. Bioinformatics
969 28:298-299.
970 Luo, R., B. Liu, Y. Xie, Z. Li, W. Huang, J. Yuan, G. He, Y. Chen, Q. Pan, and Y. Liu.
971 2012. SOAPdenovo2: an empirically improved memory-efficient short-read de
972 novo assembler. Gigascience 1:18.
973 Malpica, A. and J. F. Ornelas. 2014. Postglacial northward expansion and genetic
974 differentiation between migratory and sedentary populations of the broad-tailed
975 hummingbird (*Selasphorus platycercus*). Molecular Ecology 23:435-452.
976 Manthey, J. D. and R. G. Moyle. 2015. Isolation by environment in white-breasted
977 nuthatches (*Sitta carolinensis*) of the Madrean Archipelago sky islands: a
978 landscape genomics approach. Molecular Ecology 24:3628-3638.
979 Mayr, E. 1942. Systematics and the origin of species. Columbia Univ. Press, New York.
980 Mayr, E. 1947. Ecological factors in speciation. Evolution:263-288.
981 Mayr, E. 1954. Change of genetic environment and evolution.

982 Mayr, E. 1963. Animal species and evolution. Belknap Press, Cambridge, MA.

983 McCormack, J. E., S. M. Hird, A. J. Zellmer, B. C. Carstens, and R. T. Brumfield. 2013.
984 Applications of next-generation sequencing to phylogeography and
985 phylogenetics. Molecular Phylogenetics and Evolution 66:526-538.

986 McCormack, J. E., A. J. Zellmer, and L. L. Knowles. 2010. Does Niche Divergence
987 Accompany Allopatric Divergence in Aphelocoma Jays as Predicted Under
988 Ecological Speciation?: Insights from Tests with Niche Models. Evolution
989 64:1231-1244.

990 McKenna, A., M. Hanna, E. Banks, A. Sivachenko, K. Cibulskis, A. Kernytsky, K.
991 Garimella, D. Altshuler, S. Gabriel, and M. Daly. 2010. The Genome Analysis
992 Toolkit: a MapReduce framework for analyzing next-generation DNA
993 sequencing data. Genome research 20:1297-1303.

994 McRae, B. H. and P. Beier. 2007. Circuit theory predicts gene flow in plant and animal
995 populations. Proceedings of the National Academy of Sciences 104:19885-
996 19890.

997 Meirmans, P. G. 2015. Seven common mistakes in population genetics and how to
998 avoid them. Molecular Ecology 24:3223-3231.

999 Milá, B., P. Aleixandre, S. Alvarez-Nordström, J. McCormack, E. Ketterson, and J.
1000 Atwell. 2016. More than meets the eye: Lineage diversity and evolutionary
1001 history of Dark-eyed and Yellow-eyed juncos. Snowbird: Integrative Biology
1002 and Evolutionary Diversity in the Junco (ED Ketterson and JW Atwell, Editors).
1003 University of Chicago Press, Chicago, Illinois, USA:179-198.

1004 Milá, B., D. J. Girman, M. Kimura, and T. B. Smith. 2000. Genetic evidence for the
1005 effect of a postglacial population expansion on the phylogeography of a North

American songbird. Proceedings of the Royal Society Biological Sciences Series B 267:1033-1040.

Milá, B., J. E. McCormack, G. Castaneda, R. K. Wayne, and T. B. Smith. 2007. Recent postglacial range expansion drives the rapid diversification of a songbird lineage in the genus Junco. Proceedings of the Royal Society B-Biological Sciences 274:2653-2660.

Milá, B., T. B. Smith, and R. K. Wayne. 2006. Postglacial population expansion drives the evolution of long-distance migration in a songbird. Evolution 60:2403-2409.

Miller, A. 1941. Speciation in the avian genus *Junco*. University of California Publications in Zoology 44:173-434.

Mitton, J., Y. Linhart, J. Hamrick, and J. Beckman. 1977. Observations on the genetic structure and mating system of ponderosa pine in the Colorado Front Range. Theoretical and Applied Genetics 51:5-13.

Nadeau, N. J., A. Whibley, R. T. Jones, J. W. Davey, K. K. Dasmahapatra, S. W. Baxter, M. A. Quail, M. Joron, R. H. ffrench-Constant, M. L. Blaxter, J. Mallet, and C. D. Jiggins. 2012. Genomic islands of divergence in hybridizing Heliconius butterflies identified by large-scale targeted sequencing. Philosophical Transactions of the Royal Society B: Biological Sciences 367:343-353.

Nadeau, S., P. G. Meirmans, S. N. Aitken, K. Ritland, and N. Isabel. 2016. The challenge of separating signatures of local adaptation from those of isolation by distance and colonization history: The case of two white pines. Ecology and evolution 6:8649-8664.

Nagylaki, T. 1975. Conditions for the existence of clines. Genetics 80:595-615.

1030 Narum, S. R. and J. E. Hess. 2011. Comparison of FST outlier tests for SNP loci under
1031 selection. Molecular Ecology Resources 11:184-194.
1032 Nolan, V. J., E. D. Ketterson, D. A. Cristol, C. M. Rogers, E. D. Clotfelter, R. C. Titus,
1033 S. J. Schoech, and E. Snajdr. 2002. Dark-eyed Junco (*Junco hyemalis*) *in* A.
1034 Poole, and F. Gill, eds. The Birds of North America. The Birds of North
1035 America, Inc., Philadelphia, Pennsylvania.
1036 Nosil, P. 2012. Ecological Speciation. Oxford University Press.
1037 Nosil, P., S. P. Egan, and D. J. Funk. 2008. Heterogeneous genomic differentiation
1038 between walking-stick ecotypes:"isolation by adaptation" and multiple roles for
1039 divergent selection. Evolution 62:316-336.
1040 Ojeda Alayon, D. I., C. K. Tsui, N. Feau, A. Capron, B. Dhillon, Y. Zhang, S.
1041 Massoumi Alamouti, C. K. Boone, A. L. Carroll, and J. E. Cooke. 2017. Genetic
1042 and genomic evidence of niche partitioning and adaptive radiation in mountain
1043 pine beetle fungal symbionts. Molecular Ecology 26:2077-2091.
1044 Oksanen, J., F. Blanchet, R. Kindt, P. Legendre, and R. O'Hara. 2016. Vegan:
1045 community ecology package. R Packag. 2.3-5.
1046 Parchman, T., Z. Gompert, M. Braun, R. Brumfield, D. McDonald, J. Uy, G. Zhang, E.
1047 Jarvis, B. Schlinger, and C. Buerkle. 2013. The genomic consequences of
1048 adaptive divergence and reproductive isolation between species of manakins.
1049 Molecular Ecology 22:3304-3317.
1050 Patterson, N., A. L. Price, and D. Reich. 2006. Population structure and eigenanalysis.
1051 PLoS genet 2:e190.
1052 Poelstra, J. W., N. Vijay, C. M. Bossu, H. Lantz, B. Ryll, I. Müller, V. Baglione, P.
1053 Unneberg, M. Wikelski, M. G. Grabherr, and J. B. W. Wolf. 2014. The genomic

landscape underlying phenotypic integrity in the face of gene flow in crows. Science 344:1410-1414.

Pritchard, J. K. and A. Di Rienzo. 2010. Adaptation–not by sweeps alone. Nature Reviews Genetics 11:665-667.

Pritchard, J. K., M. Stephens, and P. Donnelly. 2000. Inference of population structure using multilocus genotype data. Genetics 155:945-959.

R_Core_Team. 2013. R: a language and environment for statistical computing. R Foundation for Statistical Computing, Vienna, Austria.

R_Studio_Team. 2015. RStudio: Integrated Development for R. R Studio, Inc., Boston, MA.

Rellstab, C., F. Gugerli, A. J. Eckert, A. M. Hancock, and R. Holderegger. 2015. A practical guide to environmental association analysis in landscape genomics. Molecular Ecology 24:4348-4370.

Riesch, R., M. Muschick, D. Lindtke, R. Villoutreix, A. A. Comeault, T. E. Farkas, K. Lucek, E. Hellen, V. Soria-Carrasco, and S. R. Dennis. 2017. Transitions between phases of genomic differentiation during stick-insect speciation. Nature Ecology & Evolution 1:0082.

Rundle, H. and P. Nosil. 2005. Ecological speciation. Ecology Letters 8:336-352.

Safran, R., E. Scordato, M. Wilkins, J. K. Hubbard, B. Jenkins, T. Albrecht, S. Flaxman, H. Karaardıç, Y. Vortman, and A. Lotem. 2016. Genome-wide differentiation in closely related populations: the roles of selection and geographic isolation. Molecular Ecology 25:3865-3883.

Schluter, D. 2000. The ecology of adaptive radiation. Oxford University Press, Oxford.

Schmieder, R. and R. Edwards. 2011. Quality control and preprocessing of metagenomic datasets. Bioinformatics 27:863-864.

1079 Seutin, G. 1991. Preservation of avian blood and tissue samples for DNA analyses.
1080 Canadian Journal of Zoology 69:82-90.
1081 Seutin, G., L. M. Ratcliffe, and P. T. Boag. 1995. Mitochondrial DNA homogeneity in
1082 the phenotypically diverse redpoll finch complex (Aves: Carduelinae: *Carduelis*
1083 *flammea-hornemanni*). Evolution 49:962-973.
1084 Slatkin, M. 1973. Gene flow and selection in a cline. Genetics 75:733-756.
1085 Soberon, J. and A. T. Peterson. 2005. Interpretation of models of fundamental
1086 ecological niches and species' distributional areas.
1087 Sork, V. L., K. Squire, P. F. Gugger, S. E. Steele, E. D. Levy, and A. J. Eckert. 2016.
1088 Landscape genomic analysis of candidate genes for climate adaptation in a
1089 California endemic oak, Quercus lobata. American journal of botany 103:33-46.
1090 Szulkin, M., P. A. Gagnaire, N. Bierne, and A. Charmantier. 2016. Population genomic
1091 footprints of fine-scale differentiation between habitats in Mediterranean blue
1092 tits. Molecular ecology 25:542-558.
1093 Templeton, A. R. 1981. Mechanisms of speciation-a population genetic approach.
1094 Annual review of Ecology and Systematics 12:23-48.
1095 Termignoni-García, F., J. P. Jaramillo-Correa, J. Chablé-Santos, M. Liu, A. J. Shultz, S.
1096 V. Edwards, and P. Escalante Pliego. 2017. Genomic footprints of adaptation in
1097 a cooperatively breeding tropical bird across a vegetation gradient. Molecular
1098 Ecology.
1099 Turner, S. D. 2014. qqman: an R package for visualizing GWAS results using QQ and
1100 manhattan plots. bioRxiv:005165.
1101 Uyeda, J. C., S. J. Arnold, P. A. Hohenlohe, and L. S. Mead. 2009. Drift promotes
1102 speciation by sexual selection. Evolution 63:583-594.

1103 Van Den Wollenberg, A. L. 1977. Redundancy analysis an alternative for canonical
1104 correlation analysis. Psychometrika 42:207-219.
1105 Vincent, B., M. Dionne, M. P. Kent, S. Lien, and L. Bernatchez. 2013. Landscape
1106 genomics in Atlantic salmon (Salmo salar): searching for gene–environment
1107 interactions driving local adaptation. Evolution 67:3469-3487.
1108 Wang, I. J. and G. S. Bradburd. 2014. Isolation by environment. Molecular Ecology
1109 23:5649-5662.
1110 Warren, D. L., R. E. Glor, and M. Turelli. 2008. Environmental Niche Equivalency
1111 Versus Conservatism: Quantitative Approaches to Niche Evolution. Evolution
1112 62:2868-2883.
1113 Wright, S. 1943. Isolation by distance. Genetics. 28:114-138.
1114 Wright, S. 1946. Isolation by distance under diverse systems of mating. Genetics 31:39.
1115 Yates, A., W. Akanni, M. R. Amode, D. Barrell, K. Billis, D. Carvalho-Silva, C.
1116 Cummins, P. Clapham, S. Fitzgerald, and L. Gil. 2016. Ensembl 2016. Nucleic
1117 acids research:gkv1157.
1118 Zheng, X. 2012. SNPRelate: parrallel computing toolset for genome-wide association
1119 studies. R package version 95.

1120

1121